Case Studies in Thermal Engineering 63 (2024) 105257

Contents lists available at ScienceDirect

Case Studies in Thermal Engineering

journal homepage: www.elsevier.com/locate/csite

Energy-economic-environmental analysis of bifacial photovoltaic thermal (BPVT) solar air collector with jet impingement

Win Eng Ewe [a], Ahmad Fudholi [b,c], Muslizainun Mustapha [d,*], E. Solomin [e], M.H. Yazdi [f], Tri Suyono [c], Nilofar Asim [b], Nurul Syakirah Nazri [g], Ahmad Rajani [c], Rudi Darussalam [c], Anjar Susatyo [c], Henny Sudibyo [c], Martoni [h], Jojo Sumarjo [i], Haznan Abimanyu [c], Kamaruzzaman Sopian [j]

[a] Energy Systems Research Unit, Mechanical and Aerospace Engineering, University of Strathclyde, Glasgow, G1 1XJ, Scotland, United Kingdom
[b] Solar Energy Research Institute, Universiti Kebangsaan Malaysia, 43600, Bangi, Selangor, Malaysia
[c] Research Center for Energy Conversion and Conservation, National Research and Innovation Agency (BRIN), Indonesia
[d] Department of Applied Physics, Faculty of Science and Technology, Universiti Kebangsaan Malaysia, 43600, Bangi, Selangor, Malaysia
[e] Department of Electric Power Generation Stations, Network and Supply Systems, Institute of Engineering and Technology, South Ural State University, 76, Lenin Avenue, Chelyabinsk, 454080, Russian Federation
[f] New Energy Research Group, New Materials Technology and Processing Research Center, Department of Mechanical Engineering, Neyshabur Branch, Islamic Azad University, Neyshabur, Iran
[g] School of Liberal Studies (CITRA), Universiti Kebangsaan Malaysia, Bangi, Malaysia
[h] Mechanical Engineering, Faculty of Engineering, Widyatama University, Indonesia
[i] Universitas Singaperbangsa Karawang, Indonesia
[j] Department of Mechanical Engineering, Universiti Teknologi PETRONAS, Seri Iskandar, 32610, Perak Darul Ridzuan, Malaysia

ARTICLE INFO

Keywords:
Bifacial solar cell
Photovoltaic thermal collectors
Environmental analysis
Economic analysis
Thermohydraulic
Electrohydraulic

ABSTRACT

Jet impingement cooling enhances photovoltaic (PV) system efficiency by using high-speed fluid jets to reduce panel temperatures, improving performance and longevity. The effectiveness depends on factors like fluid flow rate, nozzle placement, and distance from the panel. While it boosts energy output, it may increase energy use for fluid circulation and add complexity to the system. This research explores a groundbreaking approach to enhancing the efficiency of bifacial photovoltaic thermal (BPVT) systems by integrating jet impingement technology. A novel design featuring a jet plate reflector is introduced, offering the dual benefit of cooling the PV panels while simultaneously reflecting light to optimize energy capture. The study comprehensively analyses the system's performance, including energy output and a detailed techno-economic and environmental-economic evaluation. The modelling in this study was validated and reasonably consistent with experimental results. The system's output air temperature and thermal efficiency are 302.07–318.75 K and 33.83–62.28 %, respectively. The temperature and electrical efficiency range for PV systems are 304.39–339.54 K and 9.39–11.22 %. Reduced mass flow rate and increased solar irradiation are the most economically advantageous operating parameters for the proposed system, resulting in lower annual pumping costs and more significant annual energy gains for the system. CBR variations range from 0.1363 to 9.3445, with an average of 2. Additionally, by using BPVT with jet impingement to generate electricity rather than fossil fuels, it is possible to reduce annual carbon dioxide emissions by approximately 1.61 tons and save

* Corresponding author.
E-mail address: muslizainun@ukm.edu.my (M. Mustapha).

https://doi.org/10.1016/j.csite.2024.105257
Received 2 July 2024; Received in revised form 25 September 2024; Accepted 8 October 2024
Available online 11 October 2024
2214-157X/© 2024 The Authors. Published by Elsevier Ltd. This is an open access article under the CC BY license (http://creativecommons.org/licenses/by/4.0/).

RM93.51 annually. In general, the proposed method should be used to minimize environmental pollution.

1. Introduction

Energy demand has surged since the turn of the century, with fossil fuels accounting for most energy sources. Fossil fuel resources are finite and cannot be sustained for lengthy periods. The excessive use of fossil fuels significantly impacts greenhouse gas emissions and global climate change. Fossil fuels are not viable long-term energy sources [1,2]. The depletion of these resources is driven by their heavy use, leading to high greenhouse gas emissions and exacerbating global climate change [3,4]. Consequently, the demand for renewable energy alternatives has risen. An alternative energy source is essential to fulfil our energy requirements while conserving fossil resources. Solar energy, as a renewable option, could meet a substantial portion of the world's energy needs. Clean energy is produced by solar energy, which is also environmentally favourable. Solar energy is an excellent alternative for those living in rural or underprivileged areas without access to modern energy. Utilizing energy derived from renewable resources is essential to improving the current environment and offering advantages to society [5,6]. This is because renewable energy is a type of long-term energy. Solar energy is a renewable and environmentally well-disposed energy source. Photovoltaic thermal collector (PVT) systems have been extensively utilized to generate thermal energy and electricity from solar power [7,8]. This approach focuses on maximizing power generation and minimizes implementation costs. Depending on the heat transfer medium used, PVT collectors can be classified into four types: air-based, water-based, mixed (air-water-based), and nanofluid-based PVT collectors [9].

PVT collectors that use air as heat transfer fluid are called PVT air collector systems. The collector design depends on whether the airflow is single-pass or double-pass. Air circulates through a channel between the glass cover and the front PV surface or between the PV backside surface and the insulation. This circulation can occur through natural convection or forced airflow, producing hot air that can be used for heating and drying purposes. PVT systems are often integrated into building ventilation systems or combined with solar thermal collector systems. Researchers have examined the energy usage of PVT air collectors and found that the power loss factor of the system typically remains unaffected during energy efficiency evaluations. Because of this, most systems have been researched and developed in the previous few years with consideration for efficiency, economy, cost, and the environment [10,11]. Several experts claim that exergy analysis is a consistent approach to gauge the value of the economy. Energy analysis can yield the true efficiency value by evaluating the amount of system power loss. Therefore, if there is a difference between the energy efficiency evaluation and the exertion efficiency, the energy efficiency exceeds the efficiency of the previously indicated factor [12,13]. Energy analysis is one of the most complex stages of industrial design and process. This is because consuming energy as efficiently as possible is a significant concern. Exogenous value data is also essential for energy recovery, operational expenses, and various pollutants and fuels. Energy analysis is frequently used to assess solar energy systems, including PVT, solar collectors and solar drying systems [14,15].

Many researchers have studied PVT collectors. The modelling results of Bargene and Lovik [16] indicate that a PVT system's overall efficiency can range from 60 % to 80 %. Several elements are listed by Charalambus et al. [17] as influencing the performance of PVT systems, such as the absorber's thermal conductivity to the fluid interface, the absorber's plate design, mass flow rate, the working fluid's inlet temperature, and the PVT collector's overall design. Seven distinct PVT water collector designs were tested by Zondag et al. [18], who classified the designs into four categories: free flow, channel, sheet and tube, and two additional absorber types. The sheet and tube design proved the easiest to produce despite being 2 % less efficient than the channel design. Fudholi et al. [19] investigated a V-grooved PVT air collector that had been improved from an earlier V-groove design. The experimental average energy efficiency has grown from the theoretical value of 1.21 % as the contact surface between the groove and collector has increased. Furthermore, it produced an average exergy efficiency of 12.91 % theoretically and 12.66 % experimentally, concluding that the analyses were 94 % accurate when the experimental data was compared to the mathematical model of the system. An additional field study [20] revealed that a bifacial PVT solar air collector with a parallel flow design had a maximum overall energy efficiency of about 67 %. A PVT solar collector's overall efficiency can be increased by using Si-C nanofluids in a jet array; test findings show that this can lead to an electrical efficiency of 12.8 %, thermal efficiency of 85 %, and overall efficiency of 97.8 % [21]. The same authors validated their findings in a follow-up investigation using a PVT and water jet system, attaining an overall efficiency of 81 % [22].

Recent advancements in bifacial photovoltaic thermal (BPVT) collectors focus on improving efficiency and energy output [23]. Key developments include the use of jet impingement cooling for better thermal management [24]. Ewe et al. [25] developed a new energy balance equation to analyze heat transfer in a BPVT air heater with a jet plate. This study introduces dual-functional jet plate reflectors designed to provide cooling and increase light absorption on the rear side of the BPV module. The findings indicate that increasing mass flow rate enhances thermal efficiency but reduces the exit air temperature, while higher solar irradiation boosts both output air temperature and thermal efficiency. Electrically, a higher mass flow rate improves efficiency by cooling the PV panel, whereas increased solar irradiation raises the panel's temperature, lowering electrical efficiency. The study reports maximum thermal and electrical efficiencies of 51.09 % and 10.73 %, respectively. Similar authors investigated the impact of impinging air jets on the thermo-electro-hydraulic performance of BPVT systems with varying packing factors [26]. Different jet plate configurations were analyzed, with simulation results validated through experiments. Findings showed that increasing the spacing between jet holes reduces interference, improves heat transfer, and increases friction and pumping power. Hydraulic efficiency is calculated by subtracting pumping power from energy output, with the system performing best at lower Reynolds numbers. The BPVT system with 36 jet holes and optimal spacing achieved maximum thermal and electrical energy gains at critical Re values of 9929 and 5667. The system's optimal thermal, electrical, and thermo-electro-hydraulic efficiencies were 57.3 %, 10.36 %, and 83.93 %, respectively. The authors

further their studies on the effect on the exergetic performance of BPVT systems with varying packing factors [27]. The research revealed that, under optimal conditions (packing factor of 0.66, 36-hole jet plate, 900 W/m^2 solar irradiance, and 0.025 kg/s mass flow rate), the system achieved a maximum exergy efficiency of 11.88 %. The maximum exergy input, destruction, and improvement potential were 402.81 W, 345.62 W, and 304.78 W, respectively.

There is a lack of experimental research on the energy analysis of BPVT systems that incorporate jet plate reflectors. Additionally, no economic evaluations have been conducted on this topic. This research presents an experimental study on improving BPVT systems by integrating jet impingement technology. The system incorporates a unique jet plate reflector design that enhances cooling and light reflection, optimizing overall system efficiency. Besides that, using the bifacial module can increase electrical efficiency due to its ability to capture sunlight from both the front and rear sides. These modules are more effective in capturing diffuse radiation (scattered sunlight on cloudy days), which allows them to perform better in variable weather conditions compared to conventional PV modules. In addition, because of their higher efficiency, fewer bifacial panels may be needed to achieve the same energy output, which can reduce the total land area or roof space required for installation. So, the study gives a full look at the energy output as well as the technological, economic, and environmental aspects of bifacial photovoltaic thermal (BPVT) solar air collectors with jet impingement. Additionally, it examines the cost-benefit ratio, or AC/AEG, with different combinations of mass flow rate and solar intensity, allowing users to choose optimal design parameters with the lowest AC/AEG. The annual costs of reducing carbon dioxide emissions are also evaluated.

2. Energy analysis

An analytical model of one-dimensional steady-state heat flow is developed to determine the energy balance among all system components. Fig. 1 shows the heat transfer coefficients for each component of the system. An analytical model of 1-D heat flow in a steady state is created to detect the energy balance among all system factors. Energy analysis was guided according to Fig. 2 to evaluate the $\eta_{thermal}$, η_{panel}, and η_{total}. To streamline the analytical analysis, the bifacial PVT model was assumed to work as follows:

(i) Involuntary convection transfers heat beside the channels.
(ii) Along the flow path, the air heater's component and the air's convection heat transfer factors are equivalent and stay constant.
(iii) The temperatures that drop through the absorber plate, jet plate and backside plate are minor.
(iv) Assumed that all of the PV cells in the panel have the identical temperature.
(v) The bifacial panel's front and rear PV cells have similar electrical efficiency.
(vi) Airflow paths are free from leakage.
(vii) There are few thermal losses from the collector's edge.
(viii) Channels 1 and 2 have the same air mass flow rate: $\dot{m}_1 = \dot{m}_2$.
(ix) The sky is considered a black body for long-wavelength radiation.

The energy balance calculations for each system component are shown in the equations below.

i) PV laminate:

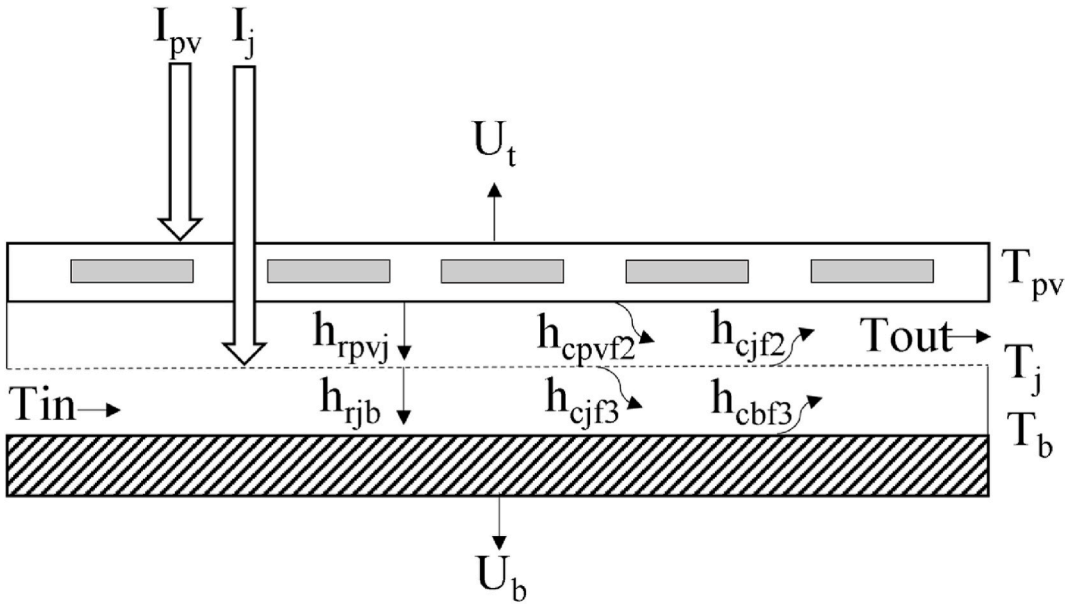

Fig. 1. The BPVT solar air collector's energy balance with jet impingement.

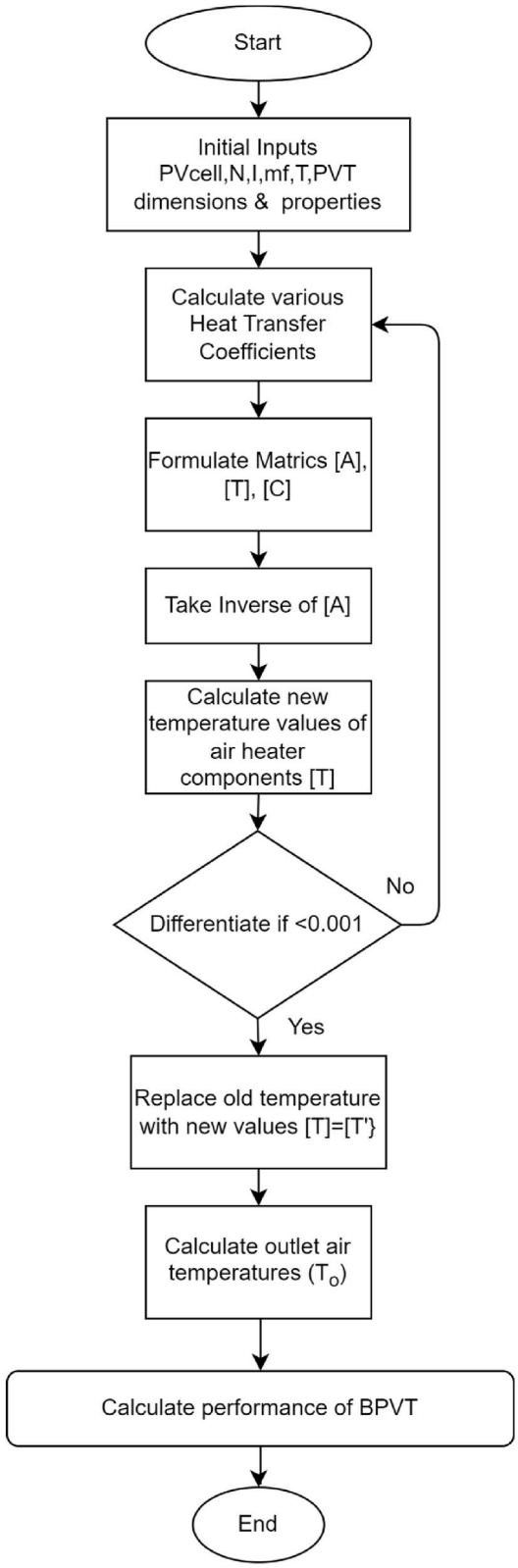

Fig. 2. Simulation flowchart of the model for BPVT.

$$I_{pv} = U_t(T_{pv} - T_a) + h_{cpvf2}(T_{pv} - T_{f2}) + h_{rpvj}(T_{pv} - T_j) \quad (1)$$

ii) Airflow among PV panel and jet plate (f2):

$$h_{cpvf2}(T_{pv} - T_{f2}) + h_{cjf2}(T_j - T_{f2}) = 2\dot{m}\mathbb{C}_p(T_{f2} - T_{f2i}) \,/\, WL \quad (2)$$

iii) Jet plate reflector:

$$I_j + h_{rpvj}(T_{pv} - T_j) = h_{rjb}(T_j - T_b) + h_{cjf2}(T_j - T_{f2}) + h_{cjf1}(T_j - T_{f1}) \quad (3)$$

iv) Airflow from the rear plate to the jet plate, f1:

$$h_{cjf1}(T_j - T_{f1}) + h_{cbf1}(T_b - T_{f1}) = 2\dot{m}\mathbb{C}_p(T_{f1} - T_{f1i}) \,/\, WL \quad (4)$$

v) Backside plate:

$$h_{rjb}(T_j - T_b) = h_{cbf1}(T_b - T_{f1}) + U_b\, x\, (T_b - T_a) \quad (5)$$

The average temperature of each channel is represented by $T_{f2} = (T_{f2i} + T_{f2o})/2$ and $T_{f1} = (T_{f1i} + T_{f1o})/2$. The temperature at the jet hole is $T_{f2i} = T_{f1o}$. The system transfers heat in two ways: (i) convective heat transfer h_c; and (ii) radiative heat transfer h_r. The channel's useable energy gain can be expressed as $2\dot{m}\mathbb{C}_p(T_f - T_{fi})/(WL)$. U_t and U_b display the heat loss from the collector's upper and back to the site. The sum of the solar radiation collected by the solar collector is expressed as $I_j = I\tau_l(1-P)(1-\eta_R)$ and $I_{pv} = I_{pvfront} + I_{pvrear}$.

Concerning the thermal energy obtained by the front bifacial PV panel,

$$I_{pvfront} = I\alpha_{pv}P(1 - \eta_{pvfront}) + I\alpha_l(1-P) \quad (6)$$

The entire quantity of heat absorbed by the front PV cell is denoted by $I\alpha_{pv}P(1 - \eta_{pvfront})$. The PV cell absorbs solar energy with a packing factor of P. The area without the PV cell is represented by (1-P), and the total heat absorbed by the front PV lamination is shown by $I\alpha_l(1 - P)$. On the other hand, the area without the PV cell is represented by $\eta_{pvfront}$ convert to electricity because $(1 - \eta_{pvfront})$ will transfer to heat.

Regarding the heat that the rear bifacial photovoltaic panel absorbs,

$$I_{pvrear} = I\tau_l(1-P)\eta_R\alpha_{pv}P(1 - \eta_{pvrear}) + I\tau_l(1-P)\eta_R\alpha_l(1-P) \quad (7)$$

Repeat Equation (1) through (5) in matrix type 5 as indicated in Equation (8) to determine the various temperatures of the solar air heater components,

$$\begin{bmatrix} A1 & -h_{cpvf2} & -h_{rpvj} & 0 & 0 \\ -h_{cpvf2} & A2 & -h_{cjf2} & 0 & 0 \\ -h_{rpvj} & -h_{cjf2} & A3 & -h_{cjf1} & -h_{rjb} \\ 0 & 0 & -h_{cjf1} & A4 & -h_{cbf1} \\ 0 & 0 & -h_{rjb} & -h_{cbf1} & A5 \end{bmatrix} \begin{bmatrix} T_{pv} \\ T_{f2} \\ T_j \\ T_{f1} \\ T_b \end{bmatrix} = \begin{bmatrix} C1 \\ C2 \\ C3 \\ C4 \\ C5 \end{bmatrix} \quad (8)$$

where,

$$A1 = U_t + h_{rpvj} + h_{cpvf2} \quad (9)$$

$$A2 = h_{cpvf2} + h_{cjf2} + 2\dot{m}\mathbb{C}_p(\mathrm{WL})^{-1} \quad (10)$$

$$A3 = h_{rpvj} + h_{cjf1} + h_{cjf2} + h_{rjb} \quad (11)$$

$$A4 = h_{cjf1} + 2\dot{m}\mathbb{C}_p(\mathrm{WL})^{-1} + h_{cbf1} \quad (12)$$

$$A5 = h_{cbf1} + U_b + h_{rjb} \quad (13)$$

$$C1 = I_{pv} + U_t T_a \quad (14)$$

$$C2 = 2\dot{m}\mathbb{C}_p T_{f2i}(\mathrm{WL})^{-1} \quad (15)$$

$$C3 = I_j \quad (16)$$

$$C4 = 2\dot{m}\mathbb{C}_p T_{f1i}(WL)^{-1} \tag{17}$$

$$C5 = U_b \, x \, T_a \tag{18}$$

The simulation code created in MATLAB can be used to calculate Equation (8) by applying the matrix inversion line, [T] = [A]$^{-1}$[C].

The upper loss coefficient (U_t) is given by:

$$U_t = \frac{1}{(h_w + h_{rpvs})^{-1}} \tag{19}$$

where $h_w = 5.7 \times 3.8(V_w)$, (20)

$$h_{rpvs} = \sigma\epsilon_{pv}(T_{pv} + T_s)({T_{pv}}^2 + {T_s}^2)(T_{pv} - T_s) \,/\, (T_{pv} - T_a) \tag{21}$$

and

$$T_s = 0.0552({T_a}^{1.5}) \tag{22}$$

The following formula provides the radiative heat transfer coefficients between a PV panel's backplate (h_{rjb}) and jet plate reflector (h_{rpvj}):

$$h_{rpvj} = \sigma(T_{pv} + T_j)({T_{pv}}^2 + T_j^2) \Big/ \left(\frac{1}{\varepsilon_{pv}} + \frac{1}{\varepsilon_j} - 1\right) \tag{23}$$

$$h_{rjb} = \sigma(T_j + T_b)(T_j^2 + {T_b}^2) \Big/ \left(\frac{1}{\varepsilon_j} + \frac{1}{\varepsilon_b} - 1\right) \tag{24}$$

The heat transfer coefficient convective between the upper channel airflow and the PV panel (h_{cpvf2}).

$$h_{cpvf2} = k \times Nu_{pvf2}/D_h \tag{25}$$

where Nusselt number, Nu_{pvf2} is given by:

$$Nu_{pvf2} = (1.658 \times 10^{-3})({Re_2}^{0.8512})\left(\frac{X}{D_h}\right)^{0.1761}\left(\frac{Y}{D_h}\right)^{0.141}\left(\frac{D_j}{D_h}\right)^{-1.9854} \times e^{\left(-0.3498 \times \left(\log\left(\frac{D_j}{D_h}\right)\right)^2\right)} \tag{26}$$

The following formula provides the convective heat transfer coefficient between the airflow in the upper (h_{cjf2}) and lower (h_{cjf1}) channels and jet plate reflector:

$$h_{cjf2} = \left(\frac{A_e}{A_c}\right) \times k \times Nu_{jf2} \Big/ D_h \tag{27}$$

$$h_{cjf1} = \left(\frac{A_e}{A_c}\right) \times k \times Nu_{jf1} \Big/ D_h \tag{28}$$

where Nusselt number, Nu_{jf2} and Nu_{jf1} is given by:

$$Nu_{jf2} = 0.0293({Re_2}^{0.8}) \tag{29}$$

$$Nu_{jf1} = 0.0293({Re_1}^{0.8}) \tag{30}$$

and the jet plate's effective heat transfer area (A_e) is determined by:

$$A_e = (A_c - N\pi{D_j}^2) + 2N_T N \tag{31}$$

The airflow in the bottom channel and the backplate's convective heat transfer coefficient (h_{cbf1}).

$$h_{cbf1} = h_{cjf1} \times \left(\frac{A_c}{A_e}\right) \tag{32}$$

U_b is the underside loss coefficient, and it is provided by:

$$U_b = k_{in}/t_{in} \tag{33}$$

D_h is the hydraulic diameter, and it is given by:

$$D_h = \left(\frac{4Wd}{2(W+d)}\right) \tag{34}$$

Re the Reynolds number, and it is provided by:

$$Re = \frac{\dot{m}D_h}{Wd\mu} \tag{35}$$

It is thought that the physical properties of air change linearly with Kelvin temperature [28]:
The viscosity of air (μ) is given by:

$$\mu = [1.983 + 0.00184(T-300)] \times 10^{-5} \tag{36}$$

The density of air (ρ) is given with:

$$\rho = 1.1774 - 0.00359(T-300) \tag{37}$$

η_{panel} can be used to calculate the system's electrical energy efficiency:

$$\eta_{panel} = \frac{P_{max}}{IA_c} \tag{38}$$

Thermal conductivity of air (k) is given using:

$$k = 0.02624 + 0.0000758(T-300) \tag{39}$$

Specific heat capacity of air (C_p) is given using:

$$C_p = 1.0057 + 0.000066(T-300) \tag{40}$$

$\eta_{thermal}$ can be used to calculate the system's thermal energy efficiency:

$$\eta_{thermal} = \frac{\dot{m}C_p(T_o - T_i)}{(I \times A_c)} \tag{41}$$

where electrical power generated (P_{max}) can be calculated with [29]:

$$P_{max} = IA_c\alpha_{pv}P(\eta_{pvfront}) + IA_c\tau_l(1-P)\eta_R\alpha_{pv}P(\eta_{pvrear}) \tag{42}$$

and frontage and back of bifacial PV efficiency, $\eta_{pvfront}$ and η_{pvrear} can be calculated by Ref. [30]:

$$\eta_{pvfront} = \eta_{pvrear} = \eta_{ref}\left(1 - B\left(T_{pv} - T_{ref}\right)\right) \tag{43}$$

For the total thermal energy efficiency (η_{total}) can be calculated by Ref. [31]:

$$\eta_{total} = \eta_{thermal} + \frac{\eta_{panel}}{0.38} \tag{44}$$

3. Economic-environmental analysis

A profitability metric called the cost-benefit ratio (CBR) is employed in cost-benefit analysis to assess the sustainability of cash flows derived from a project or asset. For instance, PVT solar collectors must gather the most solar energy at the lowest feasible cost to be economically advantageous. Therefore, it is necessary to calculate the yearly cost per unit area (AC) and annual energy gain (AEG) to evaluate the CBR of BPVT with jet impingement [32,33].

The cost-benefit ratio (CBR) in RM/m^2.kWh is given by:

$$\mathrm{CBR} = \mathrm{AC}/\mathrm{AEG} \tag{45}$$

where the annual cost per unit area (AC) in RM/year.m^2 is given by:

$$\mathrm{AC} = \mathrm{ACC} + \mathrm{APC} + \mathrm{MC} - \mathrm{ASV} \tag{46}$$

and annual energy gain (AEG) in kWh/year is given by:

$$\mathrm{AEG} = \mathrm{ATEG} + \mathrm{AEEG}/\eta_{powerplant} \tag{47}$$

For annual collector cost, ACC is given by:

$$\mathrm{ACC} = \mathrm{CI\ x\ CRF} \tag{48}$$

where the capital recovery factor (CRF), is given by:

$$\mathrm{CRF} = \mathrm{IR} \times ((\mathrm{IR}+1)^{n}) / (((\mathrm{IR}+1)^{n}) - 1) \tag{49}$$

and the capital investment (CI) is given by:

$$\mathrm{CI} = \mathrm{CPVTM} + \mathrm{CFL} + \mathrm{CSD} \tag{50}$$

where IR, n, CPVTM, CFL, and CSD are the interest rate, PV panel lifespan in years, PVT collector materials, production and labour cost, and cost of the support structure and ducting, respectively.

The maintenance cost (MC) is given by:

$$\mathrm{MC} = 10\%\ \text{of ACC} = 0.1 \times ACC \tag{51}$$

For the annual pumping cost (APC) is given by:

$$\mathrm{APC} = P_m \times \mathrm{top} \times \mathrm{CE} \tag{52}$$

where P_m, top, and CE is the mechanical pumping power, annual time of operation, and cost of electricity.

The mechanical power (P_m) needed to push air to complete the system, can be computed using [34]:

$$P_m = \frac{\dot{m} \times \Delta p}{\rho} \tag{53}$$

A pressure drop happens when there are two locations in a channel where a moving fluid has differing pressures because of friction. When a fluid passes through a tube, frictional forces brought on by the fluid's resistance to flow generate pressure dips. For the overall system pressure drop, Δp is the sum of the pressure dips in the upper and lower channels:

$$\Delta\mathrm{p} = \Delta\mathrm{p1} + \Delta\mathrm{p2} \tag{54}$$

where the pressure drop, Δp1, Δp2 can be calculated by Ref. [35]:

$$\Delta\mathrm{p1} = 2\mathrm{f}_1\mathrm{L}\mathrm{G}_1{}^2 \,/\, (\mathrm{D}_h\rho); \tag{55}$$

$$\Delta\mathrm{p2} = 2\mathrm{f}_2\mathrm{L}\mathrm{G}_2{}^2 \,/\, (\mathrm{D}_h\rho); \tag{56}$$

The Moody diagram, a non-dimensional graph used in engineering, connects the Reynolds number Re, the Darcy-Weisbach friction factor fD, and the surface roughness for fully developed flow in a circular pipe. It can, therefore predict the flow rate or pressure drop through such a pipe [36]. The friction factor is determined in this inquiry using the relevant friction factor relations from the Blassius Equation. The friction factor (f_1) for the lower ducts can be found using the following formula [37]:

$$f_1 = 0.085 \times \left(Re^{-0.25}\right) \tag{57}$$

The equation below can be used to get the upper channels (f_2) for the friction factor [10]:

$$f_2 = 0.3475 \times \left(Re^{-0.5244}\right) \times \left((X/Dh)^{0.4169}\right) \times \left((Y/Dh)^{0.5321}\right) \times \left((Dj/Dh)^{-1.4848}\right) \times exp\left(-0.2210 \times \left(\ln\left(\frac{Dj}{Dh}\right)\right)^{2}\right) \tag{58}$$

The mass velocity of air flowing through the channels, $\mathrm{G}_1, \mathrm{G}_2$ can be calculated by the following equation:

$$\mathrm{G}_1 = \mathrm{G}_2 = \dot{\mathrm{m}}/(\mathrm{W} \times \mathrm{d}) \tag{59}$$

The annual salvage value (ASV) is given by:

$$\mathrm{ASV} = \mathrm{SFF} \times \mathrm{SV} \tag{60}$$

where the salvage fund factor (SFF) is given by:

$$\mathrm{SFF} = \mathrm{IR} \,/\, ((\mathrm{IR}+1)^{n} - 1) \tag{61}$$

Table 1
The relevant data for techno-economic analysis.

Data	Assumed value
Cost of PVT materials, CPVTM	PVcell × RM8/m^2 + RM600/m^2
Cost of fabrication and labor, CFL	RM320/m^2
Cost of support structure & ducting, CSD	RM200/m^2
Cost of electricity, CE	RM0.30/kWh
Interest rate, IR	5 % or 0.05
PV panel lifespan, n	20 years
Annual time of operation (days run per annual × how many hours run per day), top	365 × 8

and the salvage value (SV) is given by:

$$\text{SV} = 10\% \text{ of CI} = 0.1 \times CI \tag{62}$$

For the annual thermal energy gain, ATEG in kWh is given by:

$$\text{ATEG} = (Qu \times \text{top})/1000 \tag{63}$$

For the annual electrical energy gain, AEEG in kWh is given by:

$$\text{AEEG} = (P_{max} \times \text{top}) \,/\, 1000 \tag{64}$$

The relevant data of BPVT with jet impingement is shown in Table 1 are used for economic analysis.

The environmental-economic analysis involves calculating the cost of annual carbon dioxide emission reductions by estimating the total energy generated from the solar system instead of fossil fuels.

For the cost of annual reduction on carbon dioxide emission, CARCDE in RM/year is given by:

$$\text{CARCDE} = \text{CFF} \times \text{ARCDE} \tag{65}$$

where the cost of fossil fuels, CFF in RM/ton CO_2, is given by Ref. [38]:

$$\text{CFF} = \text{USD } 14.5/\text{ton } CO_2 \times 4 \; (\sim \text{currency rate US Dollar to MY Ringgit}) \tag{66}$$

For annual reduction in carbon dioxide emission, ARCDE in the ton is given by:

$$\text{ARCDE} = \text{ACDE}/1000 \times \text{AEG} \tag{67}$$

where average carbon dioxide emission from fossil fuels, ACDE in kg/kWh, is given by Ref. [39]:

$$\text{ACDE} = 2 \text{ (as 2kg of } CO_2 \text{ emits for every Wh electric generateded)} \tag{68}$$

4. Experimental study

The collector comprises a bifacial PV panel, an insulated backplate, and a jet plate reflector. As seen in Fig. 3, this system also has two air channels: one between the bifacial PV panel and the jet plate reflector and the other between the jet plate reflector and the backplate. The surrounding area's air initially enters the bottom channel before passing through the jet plate reflector's holes and entering the top channel. The bottom of the bifacial solar panel is struck by air that emerges from the upper channel. The bifacial solar panel and the surrounding air exchange heat. The recommended design has the following measurements: 0.12 m in height, 0.684 m in width, and 0.703 m in length. Each airflow channel has a length of 0.025 m. The study makes use of a bifacial PV panel with packing factors of 0.22, 0.33, and 0.66 with a mass flow rate of 0.014–0.035 kg/s.

At the top of the testing portion, six rows of 48 halogen lamps each serve as solar simulators to mimic sun irradiance, according to the collector measurements. Each lamp has a 500 W heat flux and measures 118 mm in length. As illustrated in Fig. 4, solar irradiance

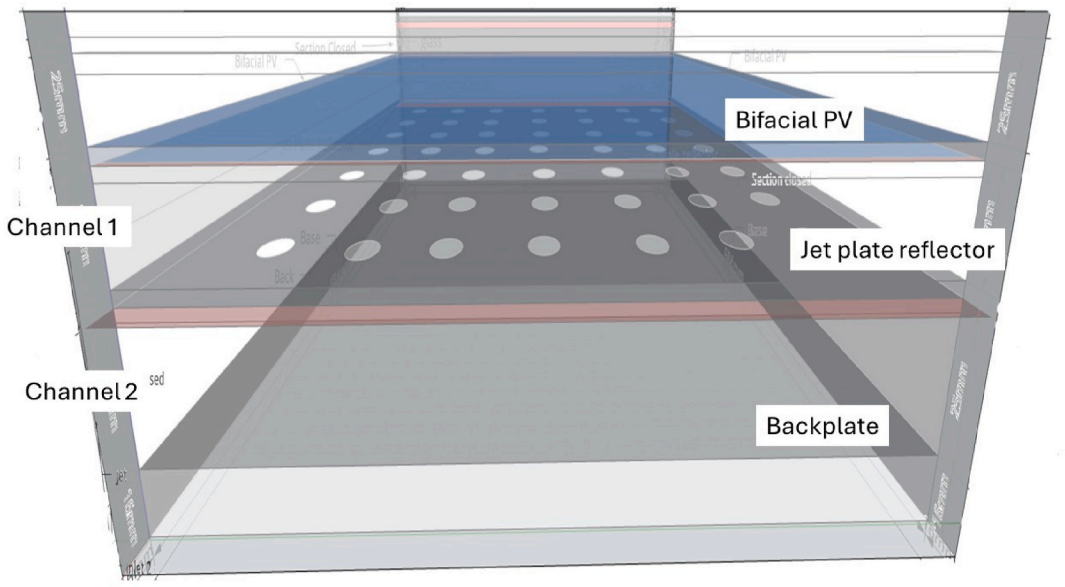

Fig. 3. Cross-sectional diagram of the BPVT with jet impingement schematically.

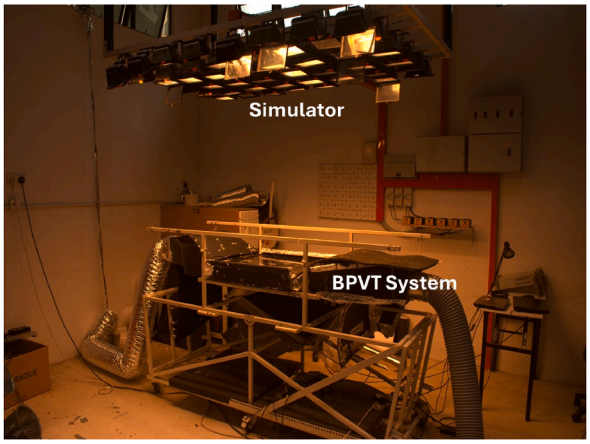

Fig. 4. Indoor experiment setup for BPVT with jet impingement.

was controlled by the digital voltage regulator. To prevent heat loss to the environment, the collector's entrance and exit are connected to manifolds or an insulated black box. Several times during the collection, temperature readings were obtained using standardized 0.2 mm K-Type thermocouples connected to an ADAM data acquisition system. An anemometer is used to measure the air wind speeds at the entrance and the outflow simultaneously. Even though forced convection mode is the main focus of the study, a blower or fan that can control the collector's needed air and heat volume is still necessary. Lastly, the I-V curve of the PV panel is measured using a DC electronic load. The protocol for the experiment was provided by Ewe et al. [26].

5. Results and discussions

This section illustrates how economic analysis with a range of design and operating aspects and energy efficiency are studied using graphical representations. Experimental results are used to validate the model findings and verify the quality of the model data. Because experimental work has limitations, the analytical inquiry is utilized for data analysis to study energy and economic analysis thoroughly. The experimental study's mass flow rate was too low to assess how well the suggested system would function in turbulent environments. The air mass flow rate's range is thus increased to 0.01–0.1 kg/s. To get the finest outcomes, the optimal operating settings are used.

5.1. Model validation

In this research method, calibration and validation are achieved by comparing the model's outputs with experimental data to ensure accuracy. The simulation algorithm, developed in MATLAB to evaluate the performance of the BPVT system with jet impingement, was validated by comparing it with experimental findings. The system, which utilized a 12-cell bifacial PV panel and a 36-hole jet plate reflector, was tested under varying mass flow rates and solar irradiation. To measure accuracy, the percentage errors between the simulated and experimental results were calculated, shown in Table 2 and Fig. 5. With accuracy rates of 94.53 % for thermal efficiency and 98.91 % for electrical efficiency, the simulation closely aligned with the experimental data, demonstrating the model's precision and reliability.

5.2. Energy analysis

Energy analysis determines the collector's thermal and electrical efficiency performance. Figs. 6 and 7 illustrate the output air

Table 2
Analysis of modeling and experimental findings for BPVT with jet impingement thermal and electrical efficiency.

$\dot{m}$ (kg/s)	I (W/m^2)	$\eta_{thermal}$			$\eta_{electrical}$			Accuracy %	
		Model	Exp.	Error (%)	Model	Exp.	Error (%)	$\eta_{thermal}$	$\eta_{electrical}$
0.014	700	40.8	38.1	7.10	10.22	10.22	0.03	92.90	99.97
	900	41.66	40.28	3.42	9.85	9.88	0.27	96.58	99.73
0.016	700	42.59	39.81	6.98	10.29	10.34	0.47	93.02	99.53
	900	43.49	41.27	5.38	9.95	10.04	0.86	94.62	99.14
0.018	700	44.14	41.14	7.30	10.36	10.48	1.11	92.70	98.89
	900	45.07	42.42	6.23	10.04	10.26	2.19	93.77	97.81
0.025	700	48.18	45.66	5.53	10.53	10.67	1.26	94.47	98.74
	900	49.22	46.65	5.51	10.27	10.44	1.62	94.49	98.38
0.035	700	51.87	49.89	3.96	10.70	10.81	1.04	96.04	98.96
	900	53.00	51.3	3.31	10.48	10.69	2.00	96.69	98.00
Avg				**5.47**			**1.09**	**94.53**	**98.91**

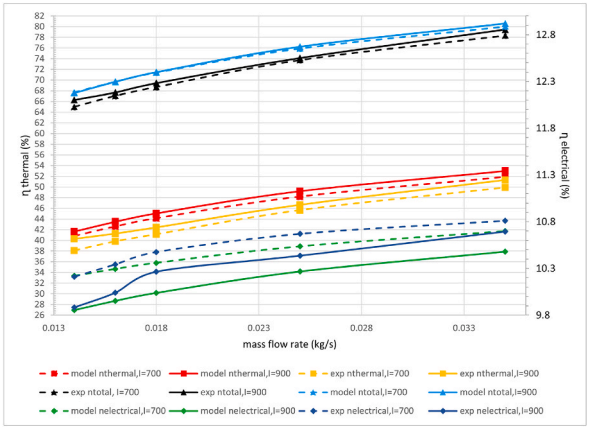

Fig. 5. Comparison of experimental results with simulation results of BPVT with jet impingement.

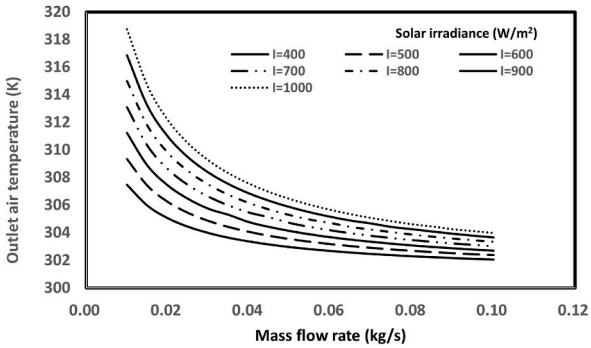

Fig. 6. Mass flow rate versus output air temperature.

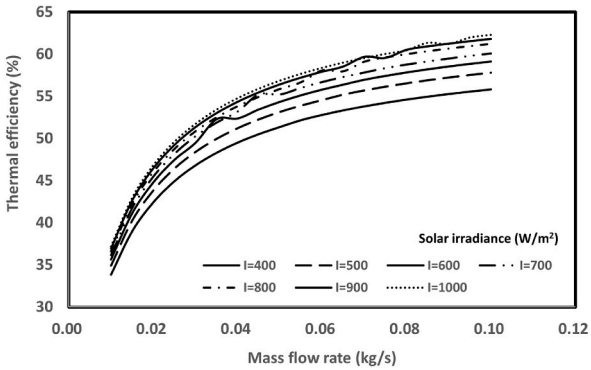

Fig. 7. The mass flow rate versus thermal efficiency.

temperature and thermal efficiency for different amounts of solar irradiation as the mass flow rate increases. Higher thermal efficiency results from improved heat transfer between the flowing fluid and the collector's parts, facilitated by a more significant mass flow rate. Moreover, a higher mass flow rate lowers the output temperature and strengthens the collector's cooling effect. As a result, when the mass flow rate increases, the collector's outlet temperature drops.

On the other hand, as solar irradiance increases, the collector's heat gain and outlet air temperature rise. Consequently, thermal efficiencies climb in tandem with the outlet air temperature. The mass flow rate and output air temperature have an inverse relationship, but it is precisely proportionate to sun irradiation. On the other hand, mass flow rate and sun irradiation directly relate to thermal efficiency. The ranges of the outlet air temperature and thermal efficiencies are 302.07–318.75 K and 33.83–62.28 %, respectively.

Figs. 8 and 9 demonstrate the PV temperature and electrical efficiency for different amounts of solar irradiation as the mass flow

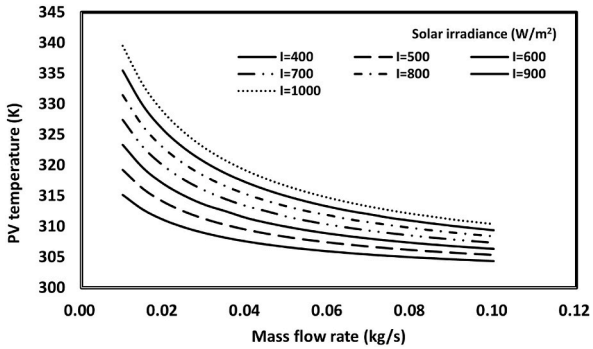

Fig. 8. Mass flow rate versus PV temperature.

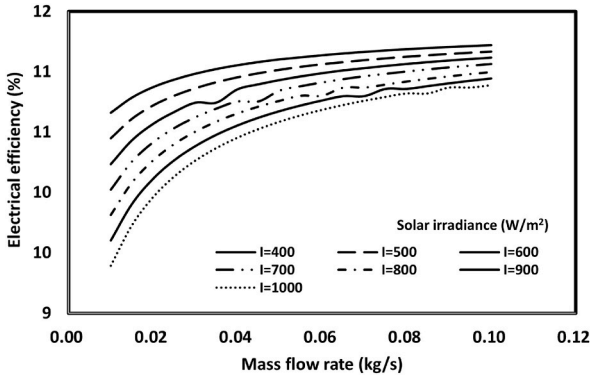

Fig. 9. Electrical energy efficiency with different mass flow rate.

rate increases. Lower PV temperatures result from a more significant cooling effect on the PV panel caused by a higher mass flow rate. The PV panel generates more electricity when it runs at a lower temperature. Consequently, when the mass flow velocity increases, the PV panel's electrical efficiency does too. Greater solar irradiation, on the other hand, will result in greater PV temperatures and worse electrical efficiency. PV temperature is directly correlated with solar irradiation but negatively correlated with mass flow ratio. By contrast, solar irradiance has an inverse relationship with mass flow rate and electrical efficiency. PV temperature ranges from 304.39 to 339.54K, while electrical efficiency ranges from 9.39 to 11.22 %.

5.3. Economic-environmental analysis

Figs. 10 and 11 show the yearly energy gain and cost-benefit ratio of the proposed system. The AEG's trend, which was directly related to mass flow rate and solar irradiation, was comparable to the thermal efficiencies. The average annual energy generation (AEG) is 806.09 kWh, with the lowest and greatest values being 347.59 and 1276.92 kWh/year, respectively. AEG adds to the CBR since AC remains constant for a comparable system with a varied mass flow rate and solar irradiance. According to the figure, higher CBR can be found at lower solar irradiance and higher mass flow rates. Hence, from the economic locus of view, lower mass flow rate and higher solar irradiance are the best operating factors for the proposed system due to lower annual pumping costs and higher annual

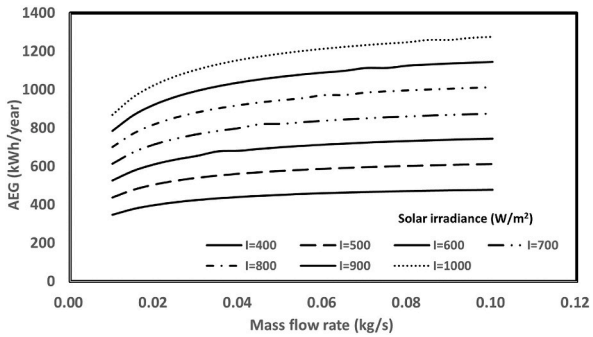

Fig. 10. AEG contrasted with mass flow rate.

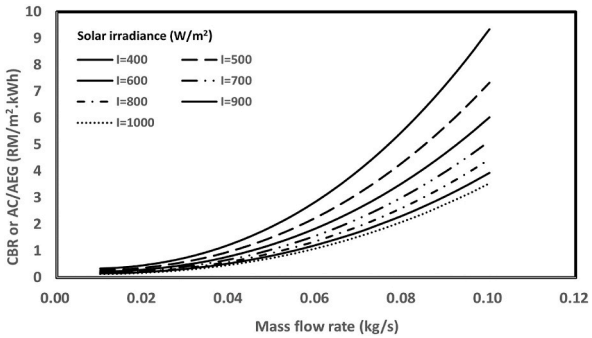

Fig. 11. CBR contrasted with mass flow rate.

energy gain. The ranges of CBR are between 0.1363 and 9.3445, with an average of 2.

Figs. 12 and 13 demonstrate the annual reduction in carbon dioxide emission and the cost of the proposed system's yearly decrease in carbon dioxide emission. A similar trend can be observed in the figures. This is because the AEG significantly impacts solar irradiation, and ARCDE and CARCDE are precisely linked to the mass flow rate. The range of ARCDE and CARCDE is between 0.6952 and 2.5539 tons/year and 40.32–148.12 RM/year, respectively, with an average of 1.61 tons/year and RM93.51/year. Hence, it can be concluded that the annual carbon dioxide emission can be reduced by about 1.61 tons, and RM93.51 can be saved annually using BPVT with jet impingement to generate energy instead of fossil fuels. Overall, the proposed system should be used to reduce environmental pollution.

6. Conclusion and recommendation

After validation, it was discovered that the modelling in this work agreed well with the outcomes of the experiments. The findings show that exit air temperature is proportional to sun irradiation, unlike mass flow rate. Conversely, thermal efficiencies are directly correlated with air velocity and solar irradiation. The system's thermal efficiency and output air temperature range from 33.86 to 32.88 % and 302.07–318.75K, respectively. Furthermore, the PV temperature has an inverse relationship with mass flow rate and a direct relationship with solar irradiation. On the other hand, there is an inverse link between solar irradiation and mass flow rate and electrical efficiency. PV systems operate within the temperature and electrical efficiency ranges of 304.39–339.54 K and 9.39–11.22 %, respectively. Therefore, a lower mass flow rate and higher solar irradiation are the proposed system's most economically cost-effective operational parameters, resulting in lower yearly pumping costs and larger annual energy gains. Regarding CBR, the variations range from 0.1363 to 9.3445, with an average of 2. Furthermore, by using BPVT with jet impingement to produce electricity instead of fossil fuels, it is possible to decrease yearly carbon dioxide emissions by about 1.61 tons and save RM93.51 annually. In general, the suggested method should be implemented to minimize environmental pollution.

The current study's goal is to evaluate experimentally and numerically the influence of jet air impingement on the thermal and electrical performance of a solar thermal collector. However, there are many critical heat transfer enhancement characteristics of jet impingement in solar thermal collectors that need to be studied, and a few recommendations for additional research were made. The following are the recommendations:

i. A CFD simulation study can be conducted to provide an extensive analytical investigation of the proposed system's performance, as this study focuses on one-dimensional steady-state analysis.
ii. Outdoor experimental work can be conducted to test the proposed system's performance in real-life climate conditions.

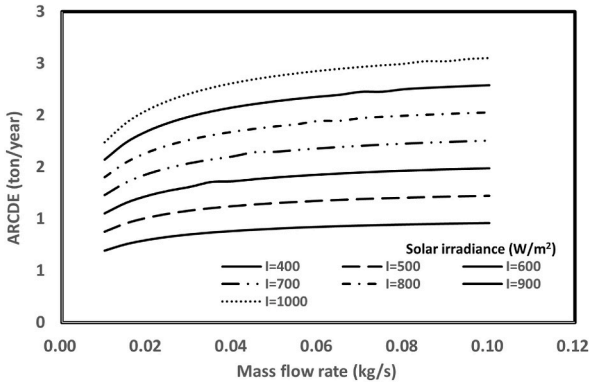

Fig. 12. ARCDE versus mass flow rate.

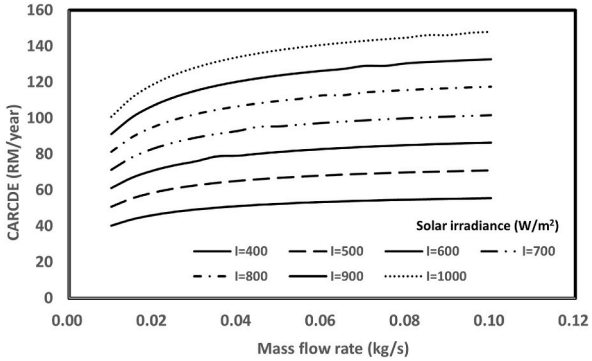

Fig. 13. CARCDE versus mass flow rate.

iii. An external reflector or Fresnel lens can be used to reflect or concentrate the solar radiation at the front side of the bifacial PV module. However, the increment of the PV temperature has to be noticed to prevent the PV module operates at high temperatures, which leads to lower electrical efficiency.

CRediT authorship contribution statement

Win Eng Ewe: Writing – original draft, Validation, Methodology, Investigation, Formal analysis, Data curation. **Ahmad Fudholi:** Writing – review & editing, Supervision, Formal analysis, Conceptualization. **Muslizainun Mustapha:** Validation, Resources, Funding acquisition, Formal analysis. **E. Solomin:** Formal analysis, Funding acquisition. **M.H. Yazdi:** Formal analysis, Funding acquisition. **Tri Suyono:** Validation, Resources, Project administration. **Nilofar Asim:** Supervision, Project administration, Formal analysis. **Nurul Syakirah Nazri:** Visualization, Formal analysis, Data curation. **Ahmad Rajani:** Visualization, Formal analysis. **Rudi Darussalam:** Resources, Funding acquisition. **Anjar Susatyo:** Resources, Funding acquisition. **Henny Sudibyo:** Project administration, Funding acquisition. **Martoni:** Resources, Funding acquisition, Resources, Funding acquisition. **Jojo Sumarjo:** Formal analysis, Funding acquisition. **Haznan Abimanyu:** Writing – review & editing, Resources. **Kamaruzzaman Sopian:** Supervision, Software, Resources, Funding acquisition, Conceptualization.

Declaration of competing interest

The authors declare that they have no known competing financial interests or personal relationships that could have appeared to influence the work reported in this paper.

Data availability

Data will be made available on request.

Acknowledgement

The authors would like to acknowledge National University of Malaysia (UKM) and Ministry of Higher Education Malaysia for research funding FRGS/1/2024/STG07/UKM/02/10.

References

[1] A. Fudholi, M. Zohri, N.S. Rukman, N.S. Nazri, M. Mustapha, C.H. Yen, M. Mohammad, K. Sopian, Exergy and sustainability index of photovoltaic thermal (PVT) air collector: a theoretical and experimental study, Renew. Sustain. Energy Rev. 100 (2019) 44–51.
[2] M. Zohri, N. Nurato, L.D. Bakti, A. Fudholi, Exergy assessment of photovoltaic thermal with v-groove collector using theoretical study, TELKOMNIKA 16 (2) (2018) 550–557.
[3] M. Zohri, S. Hadisaputra, A. Fudholi, Exergy and energy analysis of photovoltaic thermal (PVT) with and without fins collector. 2018, ARPN J. Eng. Appl. Sci. 13 (3) (2018) 803–808.
[4] M. Mustapha, A. Fudholi, K. Sopian, Mathematical modelling of bifacial photovoltaic-thermal (BPVT) collector with mirror reflector, Int. J. Renew. Energy Resour. 10 (2) (2020) 654–662.
[5] N.S. Nazri, A. Fudholi, M.H. Ruslan, K. Sopian, Mathematical modeling of photovoltaic thermal-thermoelectric (PVT-TE) air collector, Int. J. Power Electron. Drive Syst. 9 (2) (2018) 795–802.
[6] N.S. Nazri, A. Fudholi, M.H. Ruslan, K. Sopian, Experimental study of photovoltaic thermal-thermoelectric (PVT-TE) Air Collector, Int. J. Power Electron. Drive Syst. 9 (3) (2018) 1390–1396.
[7] M. Mustapha, A. Fudholi, C. Hoy Yen, M. Hafidz Ruslan, K. Sopian, Review on energy and exergy analysis of air and water based photovoltaic thermal (PVT) collector, Int. J. Power Electron. Drive Syst. 9 (3) (2018) 1367–1373.
[8] A. Fudholi, K. Sopian, R&D of photovoltaic thermal (PVT) systems: an overview, Int. J. Power Electron. Drive Syst. 9 (2) (2018) 803–810.
[9] N.S. Nazri, A. Fudholi, B. bakhtyar, C.H. Yen, A. Ibrahim, M.H. Ruslan, S. Mat, K. Sopian, Energy economic analysis of photovoltaic–thermal-thermoelectric (PVT-TE) air collectors, Renew. Sustain. Energy Rev. 92 (2018) 187–197.
[10] A. Fudholi, K. Sopian, M.Y. Othman, M.H. Ruslan, Energy and exergy analyses of solar drying system of red seaweed, Energy Build. 68 (2014) 121–129.

[11] M. Yahya, A. Fudholi, K. Sopian, Energy and exergy analyses of solar-assisted fluidized bed drying integrated with biomass furnace, Renew. Energy 105 (2017) 22–29.
[12] M.I.A. Zaini, M. Mustapha, N.N. Rosli, M.A. Mutalib, N.S. Nazri, W.M.W. Sulong, A. Fudholi, Effect of thermoelectric cooling system on the performance of photovoltaic-thermal collector: a review, Int. J. Renew. Energy Resour. 14 (3) (2024) 674–684.
[13] N.S. Nazri, A. Fudholi, E. Solomin, M. Arifin, M.H. Yazdi, T. Suyono, E.R. Priandana, M. Mustapha, M.H. Hamsan, A.H. Hussain, M.F.S. Khaidzir, M.I.A. Zaini, N. N. Rosli, M. Mohamed, K. Sopian, Analytical and experimental study of hybrid photovoltaic–thermal–thermoelectric systems in sustainable energy generation, Case Stud. Therm. Eng. 51 (2023) 103522.
[14] M. Mustapha, A. Fudholi, N.S. Nazri, M.I.A. Zaini, N.N. Rosli, W.M.W. Sulong, K. Sopian, Mathematical modeling and experimental validation of bifacial photovoltaic–thermal system with mirror reflector, Case Stud. Therm. Eng. 43 (2023) 102800.
[15] W. Mustafa, A. Fudholi, K. Sopian, M. Mustapha, Y. Ahmudiarto, The water based photovoltaic thermal fiberglass collector: an experimental investigation, Int. J. Renew. Energy Resour. 11 (4) (2021) 1663–1672.
[16] T. Bergene, O.M. Løvvik, Model calculations on a flat-plate solar heat collector with integrated solar cells, Sol. Energy 55 (6) (1995) 453–462.
[17] P.G. Charalambous, G.G. Maidment, S.A. Kalogirou, K. Yiakoumetti, Photovoltaic thermal (PV/T) collectors: a review, Appl. Therm. Eng. 27 (2) (2007) 275–286.
[18] H.A. Zondag, D.W. de Vries, W.G.J. Van Helden, R.J.C. Van Zolingen, A.A. Van Steenhoven, The yield of different combined PV-thermal collector designs, Sol. Energy 74 (3) (2003) 253–269.
[19] A. Fudholi, M. Zohri, G.L. Jin, A. Ibrahim, C.H. Yen, M.Y. Othman, M.H. Ruslan, K. Sopian, Energy and exergy analyses of photovoltaic thermal collector with ∇-groove, Sol. Energy 159 (2018) 742–750.
[20] P. Ooshaksaraei, K. Sopian, S.H. Zaidi, R. Zulkifli, Performance of four air-based photovoltaic thermal collectors configurations with bifacial solar cells, Renew. Energy 102 (2017) 279–293.
[21] H.A. Hasan, K. Sopian, A.H. Jaaz, A.N. Al-Shamani, Experimental investigation of jet array nanofluids impingement in photovoltaic/thermal collector, Sol. Energy 144 (2017) 321–334.
[22] H.A. Hasan, K. Sopian, A. Fudholi, Photovoltaic thermal solar water collector designed with a jet collision system, Energy 161 (2018) 412–424.
[23] W.E. Ewe, A. Fudholi, K. Sopian, E. Solomin, M.H. Yazdi, N. Asim, N. Fatima, G. Pikra, H. Sudibyo, W. Fatriasari, A.H. Kuncoro, C.S.A. Nandar, H. Abimanyu, Jet impingement cooling applications in solar energy technologies: systematic literature review, Therm. Sci. Eng. Prog. 34 (2022) 101445.
[24] W.E. Ewe, A. Fudholi, K. Sopian, N. Asim, Y. Ahmudiarto, A. Salim, Overview on recent PVT systems with jet impingement, Int. J. Heat Technol. 39 (6) (2021) 1951–1956.
[25] W.E. Ewe, A. Fudholi, K. Sopian, N. Asim, Modeling of bifacial photovoltaic-thermal (PVT) air heater with jet plate, Int. J. Heat Technol. 39 (4) (2021) 1117–1122.
[26] W.E. Ewe, A. Fudholi, K. Sopian, R. Moshery, N. Asim, W. Nuriana, A. Ibrahim, Thermo-electro-hydraulic analysis of jet impingement bifacial photovoltaic thermal (JIBPVT) solar air collector, Energy 254 (2022) 124366.
[27] W.E. Ewe, K. Sopian, M. Mohanraj, A. Fudholi, N. Asim, A. Ibrahim, Exergetic performance of jet impingement bifacial photovoltaic-thermal solar air collector with different packing factors and jet distributions, Heat Tran. Eng. 45 (2024) 904–914.
[28] J. Assadeg, A.H.A. Al-Waeli, A. Fudholi, K. Sopian, Energetic and exergetic analysis of a new double pass solar air collector with fins and phase change material, Sol. Energy 226 (2021) 260–271.
[29] X. Sun, M.R. Khan, C. Deline, M.A. Alam, Optimization and performance of bifacial solar modules: a global perspective, Appl. Energy 212 (2018) 1601–1610.
[30] P. Ooshaksaraei, K. Sopian, S.H. Zaidi, R. Zulkifli, Performance of four air-based photovoltaic thermal collectors configurations with bifacial solar cells, Renew. Energy 102 (2017) 279–293.
[31] J. Mohelnikova, H. Altan, Evaluation of optical and thermal properties of window glazing. 2009, WSEAS Trans. Environ. Dev. 5 (1) (2009).
[32] N.S. Nazri, A. Fudholi, B. Bakhtyar, C.H. Yen, A. Ibrahim, M.H. Ruslan, S. Mat, K. Sopian, Energy economic analysis of photovoltaic-thermal-thermoelectric (PVT-TE) air collectors, Renew. Sustain. Energy Rev. 92 (2018) 187–197.
[33] A. Fudholi, K. Sopian, M.H. Ruslan, M.Y. Othman, Performance and cost benefits analysis of double-pass solar collector with and without fins, Energy Convers. Manag. 76 (2013) 8–19.
[34] R. Karwa, S.N. Garg, A.K. Arya, Thermo-hydraulic performance of a solar air heater with *n*-subcollectors in series and parallel configuration, Energy 27 (9) (2002) 807–812.
[35] R. Karwa, K. Chauhan, Performance evaluation of solar air heaters having v-down discrete rib roughness on the absorber plate, Energy 35 (2009) 398–409.
[36] V. Sabatelli, D. Marano, G. Braccio, V.K. Sharma, Efficiency test of solar collectors: uncertainty in the estimation of regression parameters and sensitivity analysis, Energy Convers. Manag. 43 (2002) 2287–2295.
[37] S.K. Saini, R.P. Saini, Development of correlations for Nusselt number and friction factor for solar air heater with roughened duct having arc-shaped wire as artificial roughness, Sol. Energy 82 (12) (2008) 1118–1130.
[38] R. Tripathi, G.N. Tiwari, V.K. Dwivedi, Overall energy, exergy and carbon credit analysis of N partially covered photovoltaic thermal (PVT) concentrating collector connected in series, Sol. Energy 136 (2016) 260–267.
[39] C.S. Rajoria, S. Agrawal, A.K. Dash, G.N. Tiwari, M.S. Sodha, A newer approach on cash flow diagram to investigate the effect of energy payback time and earned carbon credits on life cycle cost of different photovoltaic thermal array systems, Sol. Energy 124 (2015) 254–267.